



Article scientifique

Article

2018

Accepted version

Open Access

This is an author manuscript post-peer-reviewing (accepted version) of the original publication. The layout of the published version may differ .

In-Line Seawater Phosphate Detection with Ion-Exchange Membrane Reagent Delivery

Sateanchok, Suphasinee; Pankratova, Nadezda; Cuartero Botia, Maria; Cherubini, Thomas John;
Grudpan, Kate; Bakker, Eric

How to cite

SATEANCHOK, Suphasinee et al. In-Line Seawater Phosphate Detection with Ion-Exchange Membrane Reagent Delivery. In: ACS Sensors, 2018, vol. 3, n° 11, p. 2455–2462. doi: 10.1021/acssensors.8b01096

This publication URL: <https://archive-ouverte.unige.ch/unige:114483>

Publication DOI: [10.1021/acssensors.8b01096](https://doi.org/10.1021/acssensors.8b01096)

Ion-Exchange Microemulsions for Eliminating Dilute Interferences in Potentiometric Determinations

Sutasinee Apichai, Lu Wang, Nadezda Pankratova, Kate Grudpan, Eric Bakker*

Post-review print

Sateanchok, S.; Pankratova, N.; Cuartero, M.; Cherubini, T.; Grudpan, K.; Bakker, E. "In-Line Seawater Phosphate Detection with Ion-Exchange Membrane Reagent Delivery", *ACS Sens.* **2018**, 3, 2455-2462.

DOI: 10.1021/acssensors.8b01096

In-Line Seawater Phosphate Detection with Ion-Exchange Membrane Reagent Delivery

Suphasinee Sateanchok^{‡a,b}, Nadezda Pankratova^{‡a}, Maria Cuartero^{a,c}, Thomas Cherubini^a, Kate Grudpan^b and Eric Bakker^{a*}

^a Department of Inorganic and Analytical Chemistry, University of Geneva, Quai Ernest-Ansermet 30, CH-1211 Geneva, Switzerland

^b Center of Excellence for Innovation in Analytical Science and Technology, Chiang Mai University, Chiang Mai 50200, Thailand, and Department of Chemistry, Faculty of Science, Chiang Mai University, Chiang Mai 50200, Thailand

^c Present address : Applied Physical Chemistry Division, KTH, Teknikringen 30, SE-100 44 Stockholm, Sweden

ABSTRACT: There is an urgent need for reliable seawater phosphate measuring tools to better assess eutrophication. Today, most accepted sensing approaches are based on the established colorimetric molybdenum blue assay. It requires one to modify the sample to strongly acidic conditions and to add various reagents, principally molybdate and reducing agent (e.g. ascorbic acid), to form a blue colored phosphate complex that is subsequently detected spectrophotometrically. The associated need for large sample and mobile phase reservoirs and mixing coils are, unfortunately, not ideally adapted for the development of operationally simple in situ sensing instruments. It is here demonstrated for the first time that the key reagents needed to achieve phosphate detection by the molybdate method may be delivered by passive counter transport across ion-exchange membranes. A cation-exchange Donnan exclusion membrane placed in contact with a sample flow (450 μm thick) is shown to provide the strongly acidic conditions ($\text{pH} \sim 1$) necessary for phosphate determination. Proton transport is driven, via cation-exchange, by the high sodium content of the seawater sample. Molybdate was similarly released through an anion-exchange membrane by chloride counter transport. Consequently, an in-line flow system containing the two membrane modules in series was used for delivering both hydrogen and molybdate ions into the sample to form the desired phosphomolybdate complex for subsequent spectrophotometric detection. A linear calibration graph in the range of 0.1–10 μM phosphate (3–300 ppb inorganic P) was achieved, which is sufficiently attractive for environmental work. A range of seawater samples was tested and the results from this membrane delivery device showed no significant differences compared to the classical molybdate assay chosen as the reference method.

Keywords: inorganic phosphate; molybdate assay; ion-exchange membrane; molybdate delivery; marine sensing; seawater analysis

Phosphate is a vital nutrient for all living organisms as it is needed for almost all essential biomolecules (nucleic acids, phospholipids) as well as most metabolic processes such as photosynthesis, respiration and energy delivery. It is also an important key parameter of water quality and often the limiting nutrient for the primary production in ecosystems.^{1,2} Excessive concentrations of phosphate, resulting mainly from human activity, are known to be harmful to environmental aquatic systems as they promote eutrophication.³ The monitoring and control of phosphate is urgently required for these reasons.

From the late 1960s to mid 1970s, the measurement of phosphate became an important issue to allow for a better understanding of marine systems.⁴ All phosphorus forms in the environment are transformed into their inorganic forms that are transported from terrestrial to aquatic system by natural processes including wind erosion and

leaching.⁵ Total phosphate influx into open seawater has been estimated to be in the range from 9.3×10^{10} mol/year to 34×10^{10} mol/year.⁶ Phosphate concentration depends on the specific marine environment and depth. Vertical profiling of phosphate concentration in the North-East Atlantic gave concentrations below 2.5 μM .⁷ A depth profile of phosphate in the eastern mediterranean was gave less than 0.25 μM in surface waters, but nutrient sinking increased this to 10 μM at higher depth.⁸ In another study in deep seawater (321 m depth) of Toyama Bay, Japan, a significant daily phosphate changes were observed from 0.86 to 1.98 μM .⁹

Established techniques for phosphate determination commonly used in routine analysis include colorimetry, ion chromatography and flow injection analysis.^{1,4} The standard method for the determination of soluble phosphate is colorimetry by the molybdenum blue reaction (MB). By far

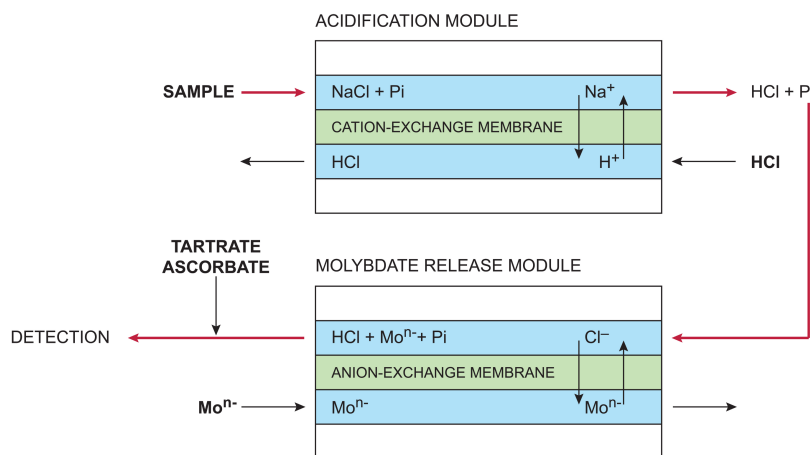


Figure 1. Membrane principles for the in-line acidification module based on cation exchange (acidification module) and anion exchange (molybdate release module), Pi: phosphate species, Mo^n : Molybdenum anion.

the most widely-used reduction method for batch and automated analyses is based on the approach described by Murphy and Riley.^{10,11} It asks for ascorbic acid to reduce the phosphomolybdate complex in the presence of potassium antimony tartrate as catalyst in acidic medium. The reaction pH and the molybdate concentration are key parameters for the formation of the phosphomolybdate complex and for controlling its reduction. The best sensitivity for orthophosphate detection occurs at a $\text{pH} < 1$.¹²⁻¹⁴

In the past few years increased attention has been given to the implementation of the molybdenum blue reaction in flow analysis for determining phosphate in aquatic systems. The currently available flow methods involving flow injection analysis (FIA), segmented flow analysis (SFA), and sequential injection analysis (SIA) often provide sufficiently low detection limits for the analysis of natural seawater samples. The FIA methods are typically coupled to UV-VIS spectrophotometry, ICP-AES detection and fluorometric or chemiluminescence detection.^{1,10} Special care in sample and reagent delivery and stability is required for reliable performance.^{15,16} Despite the wide acceptance of MB-based spectrophotometric methods, they are still rather cumbersome for field monitoring applications: they involve high cost, operational complexity, high energy consumption, and require sample pre-treatment, reagent additions and storage.^{1,17} For these reasons, the development of systems for in-situ phosphate determination is an important research direction for the advancement of environmental science and conservation.⁶ Recent research by the group of V. Garçon suggested a new approach based on the electrochemical generation of molybdate by the oxidation of a molybdenum electrode and electrochemical release of hydrogen ions through a cation-exchange membrane, followed by electrochemical detection of the resulting complex.¹⁸ While this elegant research is still in the early stages, it forms an important step towards achieving a miniaturized and simplified phosphate sensing assay.

Ion-exchange membranes are established in fuel cells and in a range of analytical instrumentation such as ion suppressors in ion chromatography¹⁹ and, more recently, as electrochemical desalinators²⁰ and potentiometric probe materials.¹⁷ They are an attractive means to deliver reagents as they allow to avoid sample dilution and the use of complex mixing valves and pumps, thereby greatly

simplifying the instrument. While they are chemically robust, their ion-exchange selectivity is limited and their applicability as analytical tools must be carefully evaluated for the sample matrix of interest. The use of proton-exchange membranes for the acidification of the sample plug has been well-established in the past with ion suppressors in ion chromatography. A few new approaches based on ion-exchange membranes have been suggested recently.^{18,22}

We report here on the use of cation- and anion-exchange membranes for realizing an elegant and simplified approach to phosphate determination in seawater samples. The key reagents (molybdate anions and hydrogen ions) are delivered separately into the sample by diffusional counter transport across ion-exchange membranes (Figure 1). The phosphomolybdate complex formed in this manner is spectrophotometrically detectable, as done here, but may in principle also be measured electrochemically.²³ The proposed setup is based on a flow configuration and is therefore compatible with integration in a submersible module for subsequent in-situ determinations, similar to other systems described recently.²⁴ The suggested approach is therefore less complex than those based on classical mixing of reagent streams and likely easier to accomplish compared to the concept suggested by Garçon et al., as the reagent delivery is being achieved under zero-current conditions, by passive diffusion.

EXPERIMENTAL

Reagents. Sodium chloride (NaCl), sodium phosphate monobasic (NaH_2PO_4), potassium chloride (KCl), ammonium molybdate tetrahydrate ($(\text{NH}_4)_6\text{Mo}_7\text{O}_{24} \cdot 4\text{H}_2\text{O}$), sodium molybdate dihydrate ($\text{Na}_2\text{MoO}_4 \cdot 2\text{H}_2\text{O}$), L-ascorbic acid ($\text{C}_6\text{H}_8\text{O}_6$), potassium antimonyl-tartrate trihydrate ($\text{C}_8\text{H}_4\text{K}_2\text{O}_{12}\text{Sb}_2 \cdot 3\text{H}_2\text{O}$), sodium hexafluorosilicate (Na_2SiF_6), hydrochloric acid (HCl, 37%), concentrated sulfuric acid (H_2SO_4 , 96%) were purchased from Sigma-Aldrich (analytical grade). Aqueous solutions were prepared in deionized water ($>18 \text{ M}\Omega \text{ cm}$). The artificial seawater sample for a standard calibration was purchased from NEPTUNE SA (Aquarium shop in Conignon). The seawater samples were sourced from select locations in France and Italy. The following samples were from Arcachon Bay, a triangular-shaped shallow lagoon

close to the Atlantic coast of France: La Hume (sample 1) was sampled at a depth of 3 m, position at 44.3975 °N, 1.06709 °E, water temperature 17.5 °C, salinity 32.6 PSU. Arcachon Har-16.5 °C, salinity 31.8 PSU. Le Tés (sample 3), was taken from a depth of 1 m, position at 44.3924 °N, 1.08834 °E, water temperature 17 °C, salinity 33.5 PSU. An additional sample was from Genoa Station, Italy (sample 4), one of the major ports of the Mediterranean on the northwestern coast of Italy. It was collected from a depth of 4 m, position 44.23 °N, 8.55 °E, salinity 37.2 PSU. All collected samples were immediately stored in a cold box and finally in a fridge at 4 °C before phosphate analysis, pH was around 8. Silicone rubber for the solution channels (Angst + Pfister) was purchased from APSOparts®.

Acidification and molybdate-releasing modules. Cation-exchange membrane FKL-PK-130 (thickness 110-140 µm) and anion-exchange membranes FAB-PK-130, FAS-PET-130, FAD-PET-75 and FAPQ-375-PP (thicknesses 110-130, 110-130, 70-80 and 70-80 µm respectively) were purchased from Fumatech® (FuMA-Tech GmbH, Germany). The membranes were cut in pieces of 6×110 mm (for the acidification/molybdate module). The FKL membranes were pre-conditioned in deionized water for at least 6 h at room temperature and then at least 1 day in 1 M HNO₃ to ensure complete saturation of the membrane with hydrogen ions. The anion-exchange membranes were pretreated as per supplier recommendations: the FAB, FAS and FAD membranes were pre-conditioned in 100 mM NaCl (overnight), the FAPQ membranes need no pre-conditioning and were mounted dry in the module directly after cutting.

The design of the acidification and molybdate-releasing modules is identical to the one reported earlier for the acidification cell²² and is illustrated in Figure S1. The cell consists of a sheet of cation- or anion-exchange membrane placed between two rubber channels (rubber: 10 × 119 × 0.45 mm, channel: 1.7 × 100 × 0.45 mm). One rubber was prepared for the sample and the other for the acid solution (acidification module, H-module) or molybdate solution (molybdate module, Mo-module). These elements are in turn placed between two acrylic blocks (30 × 120 × 14 mm) and tightly closed by screws. The ends of the channels coincide with the inlet and outlet of each block. The inlets and outlets of the two blocks of each module are placed in reverse order to provide counter flow in the two channels.

Voltammetric experiment with paper-based cell. The paper-based electrochemical flow cell has been mounted according to Cuartero et al.²⁵ The elements of the cell were placed in the following order: the silver foil (working electrode [WE]), first filter paper, the anion-exchange membrane, the second filter paper, and the silver/silver chloride foil (reference [RE]/counter electrode [CE]). The elements were tightly squeezed together between two acrylic blocks. Both paper-channels were cut from Whatman filter paper (90-mm diameter, 8-µm pore size, 190-µm thickness, purchased from Sigma-Aldrich). The ends of paper-channels were dipped into two separate beakers with aqueous solutions (Solutions 1 and 2) containing either 100 mM NaCl or 100 mM Na₂MoO₄, thus obtaining the following cell: Ag|AgCl|Solution 1|membrane| Solution 2|Ag. Two special tape masks were added to the system on

bour center (sample 2) was collected at a depth of 3 m, position at 44.39652 °N, 1.0905 °E, water temperature

both sides of the membrane in order to ensure that the two filter papers do not come in contact with each other.

Membrane selectivity of molybdate-releasing module. Aqueous solutions were prepared by dissolving the appropriate salts in deionized water. FAPQ membrane was cut in the size of 7 mm diameter and mounted in OSTEC bodies (Oesch Sensor Technology AG, Sargans, Switzerland). A membrane disk was conditioned in 0.6 M NaCl overnight. The inner compartment of the Ostec electrode bodies was also filled with 10 mM NaCl. Solutions of Cl⁻ (NaCl), H₂PO₄⁻ (NaH₂PO₄) and MoO₄²⁻ (Na₂MoO₄) were used to evaluate the selectivity of membrane. Potentiometric experiments were performed against a double-junction Ag/AgCl/sat. KCl/1 M LiOAc reference electrode. Membrane selectivity was evaluated by adding aliquots of salts into water and the selectivity coefficients were calculated using the separate solution method.²⁶ To do so, the obtained separate calibration curves were extrapolated to 1 M and the selectivity coefficient was calculated from this potential difference dividing by the theoretical slope (59.2 or 29.6 mV for singly- and doubly-charged anions, respectively). The activity of the ion was calculated with a two-parameter Debye-Huckel approximation and the speciation of phosphate and molybdate was calculated for each concentration from the experimental pH value.

Colorimetric measurement procedure. The spectrophotometric detection of phosphate was based on molybdenum blue (MB) reaction described by Strickland and Parsons.¹² The ammonium molybdate solution (S_{molybdate}) was obtained by dissolving 15 g of ammonium molybdate tetrahydrate in 500 mL of water. The sulfuric acid solution (S_{acid}) was prepared by adding 140 mL of concentrated sulfuric acid (96%) in 900 mL of water. Ascorbic acid solution (S_{ascorb}) was prepared by dissolving 27 g of L-ascorbic acid in 500 mL of water and stored in the freezer overnight and whenever not in use. Potassium antimony tartrate solution (S_{antimony}) was obtained by dissolving 0.34 g of potassium antimonyl-tartrate trihydrate in 250 mL of water. Finally, the freshly mixed reagent for phosphate detection (Reagent^(P)) was prepared the same day as the colorimetric analysis to be performed, by mixing the solutions described above in the following volumetric ratio: S_{molybdate}: S_{acid}: S_{ascorb}: S_{antimony} = 2:5:2:1. The mixed reagent was added to the sample in a volumetric ratio of 1:10 (reagent:sample) for classical colorimetric analysis.

The spectrophotometric detection of molybdate has been achieved in a similar manner using Reagent^(Mo) with the composition similar to Reagent^(P) containing no molybdate but 10 mM total phosphate instead (added as sodium phosphate monobasic), to make molybdate the limiting reagent in the milimolar range.

Spectrophotometric detection was performed with a UV/VIS spectrophotometer (Lambda 35, Perkin Elmer, USA) in a flow-through quartz cell with the light path of 10 mm and a 30 µL volume (Perkin Elmer, USA, part N B0631090), at a wavelength of 660 nm. The baselines were recorded with artificial seawater. Importantly, whenever manual addition of the reagents was used, the time inter-

vals between spiking the reagent and the analysis were kept constant and identical to those used for calibration protocol (ca. 30 min, considering ca. 13 min flow path to the detector in the chosen setup).

In-line phosphate detection. The experimental setup for phosphate determination is shown in Figure S2. The solution was delivered by peristaltic pumps (ISMATEC, Model ISM935c, Clattbrug, Switzerland) equipped with tygon tubings (ISMATEC, inner diameter 1.42 mm). Two pumps were used to allow for the delivery of solution streams at identical flow rates ($90 \mu\text{L min}^{-1}$). The solutions were pumped through at four different positions (A-D). The tygon tubings installed on the pumps were connected to the flow path using PTFE tubings (BOLA, inner diameter 0.8 mm). The used reagents (hydrochloric acid and sodium molybdate from the ion-exchange modules) and the analyzed solutions from the system were collected in waste bottles.

To obtain the calibration traces, sample solutions with different phosphate concentrations were introduced by a peristaltic pump (flow rate $90 \mu\text{L min}^{-1}$). The solution at the inlet of the system was changed every 10 min by switching from the sample to the calibrant solution and the baseline (artificial seawater). These sequential solutions were passed through the in-line configuration containing the molybdate module and acidification module, respectively. An acid concentration of 5-6 M and 6 mM of molybdate were fed into the H-module and Mo-module, respectively. The stream of the resulting solution containing the phosphomolybdate complex was merged and mixed with an excess of reducing reagent (mixed solution Reagent^(R) of Sascorb and Santimony at the same ratio as colorimetry by standard spectrophotometry⁷) via a mixing coil. The resulting absorbance was recorded as a function of time by spectrophotometry at a 1-s time interval. After each experiment (involving three repetitions), the baseline solution was flushed through the system for 20 (or 15) min after every phosphate-containing solution, in order to eliminate any baseline drift.

RESULTS AND DISCUSSION

This work explores the use of ion-exchange membranes to deliver hydrogen and molybdate ions to seawater samples with the goal to achieve an instrumentally simpler phosphate measurement. While sample acidification by ion-exchange has been established in the past,¹⁸ the release of molybdate anions into the sample by chloride counter transport across an anion-exchange membrane has not yet been reported. A previous study has explored a range of anion-exchange membranes as anion-responsive membranes in potentiometry,²³ and similar materials were explored here: FAB-PK-130, FAS-PET-130, FAD-PET-75, and FAPQ-375-PP.

Voltammetric experiments were performed to assess the anion transfer characteristics across these four membranes, using a paper-based cell similar to the one reported previously (see experimental section).²⁵ This cell contains Ag (WE) and Ag/AgCl (CE/RE) elements, each in contact with a NaCl solution in a paper-based channel with a thickness of $190 \mu\text{m}$. The two solutions are separated by the anion-exchange membrane. Linear scan voltammetry

starts oxidizing silver on one of the elements to AgCl, thereby removing chloride from the contacting sample. The opposite electrode undergoes the opposite reaction, resulting in a net chloride flux across the anion-exchange membrane.

The cyclic voltammograms (CVs) obtained using all four different types of anion-exchange membranes were compared to those observed in the same paper-based cell but with no membrane between two paper-based channels (see Figure S3). Well-pronounced symmetric cathodic and anodic peaks, with the peak current decreasing with the addition of the anion-exchange membranes into the system, suggest that the overall process must be limited by diffusion. While the peak current decrease indicates to some extent less efficient ion transport, the decreasing slope in the linear range of the CVs (no membrane > FAS~FAD > FAPQ > FAB) mainly accounts for increasing resistance (minimal resistance with no membrane). No clear cathodic/anodic peaks are observed for the FAB-based system which exhibits the lowest current density (inefficient ion transport) and a purely resistive current response.

Despite the higher current density in the voltammograms with FAS and FAD compared to FAPQ, the latter was chosen for the further transport experiments. The choice of the FAPQ membrane was dictated as well by the other physico-chemical properties of the membranes (provided by the supplier Fumatech®): the FAS membrane pH stability range (from 0 to 8) is not sufficient for environmental applications as the pH of open-sea seawater normally ranges between 7.5 and 8.4,²⁷ while the FAD membrane was not chosen for mechanical reasons as the initially flat and relatively thin FAD membrane ($75 \mu\text{m}$) was found to distort and twist upon conditioning. The latter made it too difficult to integrate it between two acrylic modules of the anion-exchange module. In contrast, the FAPQ membrane does not require pre-conditioning, which makes it very easy to integrate into the module and its pH stability range (0-10) is also sufficient for the desired application.

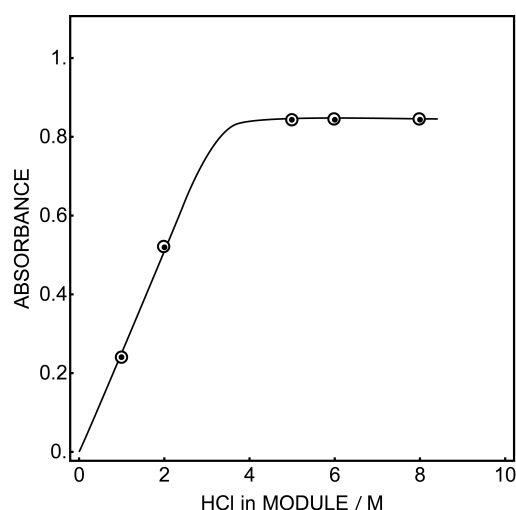


Figure 2. Effect of acidity on color intensity ($n=3$) for a sample containing $100 \mu\text{M}$ phosphate. Explored HCl concentrations were in the range of 1-8 M. Absorbance meas-

urement by spectrophotometer is obtained at 660 nm. All lines are shown to guide the eye.

The possibility of passive molybdate release through FAPQ membrane was confirmed by a simple visual colorimetric experiment. The paper-based cell was newly assembled but this time NaCl in the second compartment (Compartment 2, adjacent to Ag/AgCl element) was substituted by 100 mM sodium molybdate solution. The cell

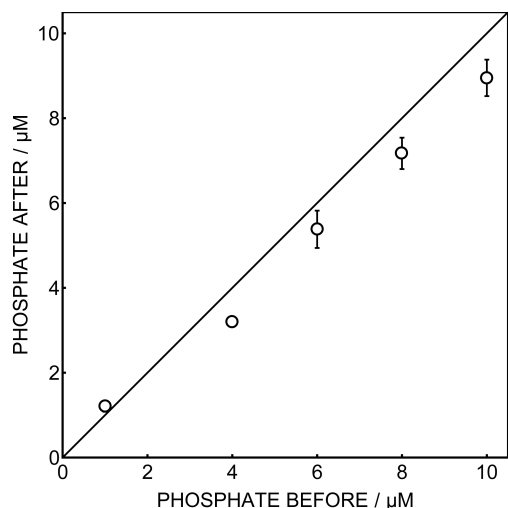


Figure 3. Correlation graph between phosphate concentrations after passing through membrane modules, including molybdate module and acidification module, and in sample initially ($n=3$). Linear line is plotted to guide a linear trend.

was dismantled after ca. 30 min to ensure that there was enough time given for the liquid to reach the top of the filter paper and for the expected anion exchange to happen. A few drops of the colorimetric reagent Reagent^(Mo) were deposited on top of both papers. The intensive blue coloration of both papers from both compartments of the cell was detected visually, confirming the efficient transport of molybdate anions through the FAPQ membrane. The same experiment was repeated with the FAB membrane, but no coloration was observed after dropping the reagent on the paper-channel dipped into sodium chloride solution. Thus, the FAB membrane was again shown not to be applicable for the anion transport in the chosen system.

After having completed the comparative studies, the FAPQ anion-exchange membrane was mounted into an ion-exchange module of in-line configuration, similar to the one previously reported for in-line sample acidification¹⁸ (Figure S1). The efficiency of molybdate transport through the FAPQ membrane was evaluated by a colorimetric molybdate assay in the excess of phosphate (Figure S4), using the calibration line (Figure S4a) obtained by passing molybdate calibration solutions with 0.6 M NaCl background through the colorimetric flow cell directly after spiking the Reagent^(Mo). Samples containing 0.6 M NaCl background were passed through the anion-exchange membrane module with different molybdate concentration in the feed and subsequently analysed in the spectrophotometric cell

after appropriate spiking with the mixed reagent Reagent^(Mo). As shown in Figure S4b, the observed linear correlation between resulting molybdenum concentration in the receiving sample solution (at the outlet of the anion-exchange module) and its concentration in the feed solution allows one to calculate the molybdate delivery efficiency for the chosen conditions as 70-75 %.

An in-line acidification approach based on passive hydrogen ion transfer through a cation-exchange FKL membrane has been recently proposed in our group to adjust the pH of freshwater samples for nitrite detection.²² Previous studies with such cation-exchange membranes showed that they are sufficiently impermeable to anions²⁸ and therefore should allow one to maintain the same phosphate concentration in the sample plug after passing through the acidification module. This custom-built module was adapted for the assay of phosphate, see Figure S1.

The current study refers to phosphate detection in seawater, which contains a high concentration of sodium chloride (ca. 0.6 M). This high concentration forms a strong diffusional driving force for membrane exchange with hydrogen ions. In order to enable the detection of phosphomolybdate complex, a final pH of <1 is required after acidification. The suitable acid concentration in the acidification module was determined by passing 100 μM phosphate solution in 0.6 M NaCl background through the molybdate module (3 mM Na_2MoO_4) and the acidification module with different acid concentrations (HCl 1-8 M). The colour intensity of blue product was analysed colorimetrically after spiking reducing reagent (Reagent^(R)). The correlation graph is shown in Figure 2 and suggests that optimal performance is observed with 5-6 M HCl, giving a final pH in the sample plug of ca. 0.85-1.00. The same membrane was used for at least three weeks without significant deterioration of the analytical performance.

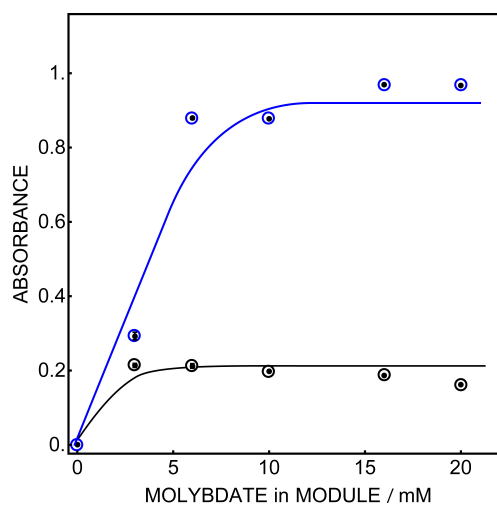


Figure 4. Effect of molybdate reagent on color intensity for phosphate determination: standards containing 100 μM (blue circles) and 10 μM (black circles) phosphate. The explored molybdenum concentrations were in the range of 0-20 mM. The absorbance of the blue complex obtained was measured by spectrophotometer at 660 nm.

After choosing the optimal HCl concentration, the anion-exchange (molybdate-releasing) and the cation-exchange (acidifying) modules were coupled in series (see Figure S2). To make sure that no molybdate loss occurs while passing the sample through the cation-exchange module, a sample containing 2 mM Na_2MoO_4 and 0.6 M NaCl background was passed through the H-module. The liquid sampled at the outlet of the sample compartment was spiked with Reagent^(Mo) containing all components with the exception of acid (as the sample had been sufficiently acidified by the membrane module) and was analysed colorimetrically. The same manipulation was performed with the sample containing 3 mM Na_2MoO_4 and 0.6 M NaCl after passing through both modules (Mo- then H-module). The results of the described two experiments are shown as gray and black circles in Figure S4a: the resulting molybdate concentrations are close to the expected 2 mM value (expected value predicted from the correlation shown in Figure S4b). The slightly elevated concentration obtained for the sample having passed through both Mo- and H-modules accounts most probably for the slightly different pH between the calibration solutions and the sample, because for the latter acidification was done by membrane transport. The results confirm no visible losses of molybdenum in the acidifying module. This is expected, as anionic molybdenum species are unlikely to permeate through cation-exchange membrane.

In contrast, the anion-exchange membrane used for molybdate delivery may allow for some passage of other anions such as phosphate. The potential loss of phosphate in the anion-exchange module was therefore evaluated. The anion selectivity of the FAPQ membrane was assessed by potentiometry. The membrane responded to Cl^- with a Nernstian slope of 59.12 mV, similar as traditional ion-selective electrode membrane, see Figure S5b. No significant membrane selectivity was observed for chloride over phosphate, with $\log K_{\text{Cl},\text{H}_2\text{PO}_4}^{\text{pot}} = -1.12 \pm 0.25$ (Figure S5a). However, the concentration of NaCl in seawater (~0.6 M) is significantly higher than that of phosphate (sub- μM range). This suggests that the exchange of molybdate anions from the feed solution will be mainly accompanied by chloride counter transport, thereby suppressing loss of phosphate from the sample.

The extent of phosphate loss was studied by a standard colorimetric phosphate assay for varying levels of phosphate in a 0.6 M NaCl background before and after passage through the combined acidification and molybdate modules. Figure 3 shows the resulting correlation of phosphate concentration obtained from the two experiments. The loss of phosphate was indeed not dramatic, on the order of 10%, and might also be caused by processes other than membrane transport. The determined phosphate concentration may be corrected for the loss if needed, provided that the experimental conditions remain sufficiently similar between calibration and measurement.

Optimization of the experimental conditions was performed before turning to seawater measurements. Phosphate calibration curves (0–100 μM) were recorded at different flow rates, see Figure S6. A higher flow rate is known to decrease the residence time and therefore the dispersion of mixed solution zone, providing a narrower peak sig-

nal.²⁹ This, however, may be at the expense of a decreased sensitivity owing to incomplete ion exchange by the membrane module and insufficient reaction time. From the data shown in Figure S6, a flow rate of 90 $\mu\text{L min}^{-1}$ was selected as each solution gave good separation.

The volume of the sample plug also affects the separation. It is controlled by the injection time via the preselected flow rate. Here, 5, 10 and 15 min injection times gave 0.45, 1.00 and 1.35 mL sample volumes. Figure S7 shows the corresponding results for a range of phosphate concentrations (0–50 μM), suggesting that 1 mL is suitable as each phosphate concentration can be clearly separated.

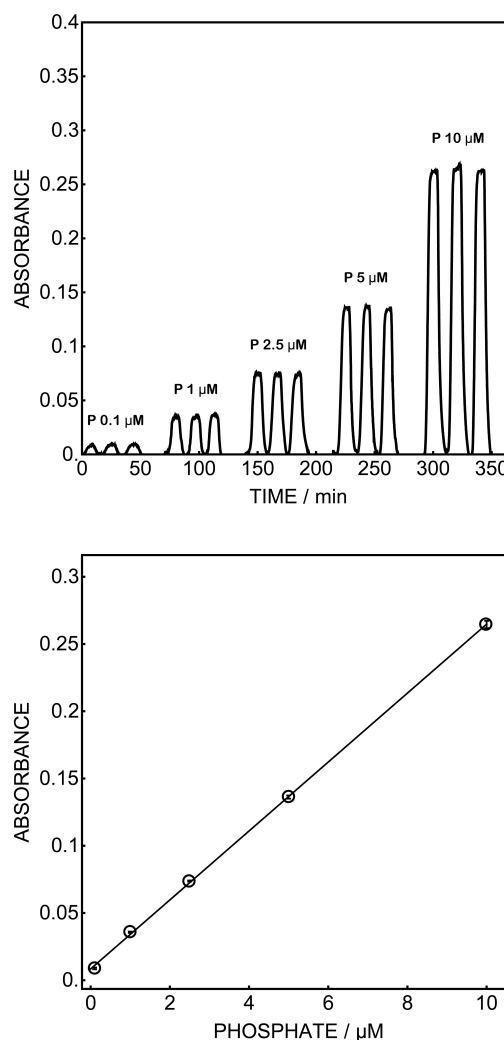


Figure 5. Top: Time-dependent signals for different phosphate concentrations (0.1–10 μM). Bottom: Corresponding calibration graph from the time-based data (error bars are standard deviations; $n=3$), volume of sample plug ca. 1 mL. Absorbance is measured at 660 nm.

The concentration of molybdate in the Mo-module was varied to study the influence on system performance. Most literature ask for a molybdate concentration in the millimolar range.¹⁰ Consequently, the range of explored concentrations in the reagent solution was 0–20 mM, see Figure 4 and Figure S8 for results. The absorbance of the blue product was analysed colorimetrically after spiking redu-

cing reagent (Reagent^(R)). Two phosphate standards, with 100 μM (blue line) and 10 μM (black line) phosphate concentrations, were analyzed in the suggested setup with different molybdate concentrations and a 5 M HCl acid concentration in the feed streams. The sensitivity of the method was found to increase with increasing molybdate concentration up to 6 mM, after which it was constant. For this reason, a 6 mM molybdate reagent concentration was chosen in the reagent stream of the Mo-module.

Seawater samples were analyzed for phosphate by guiding the sample plug first through the acidification module and subsequently through the molybdate-releasing module. While the ultimate goal of the work is to achieve an

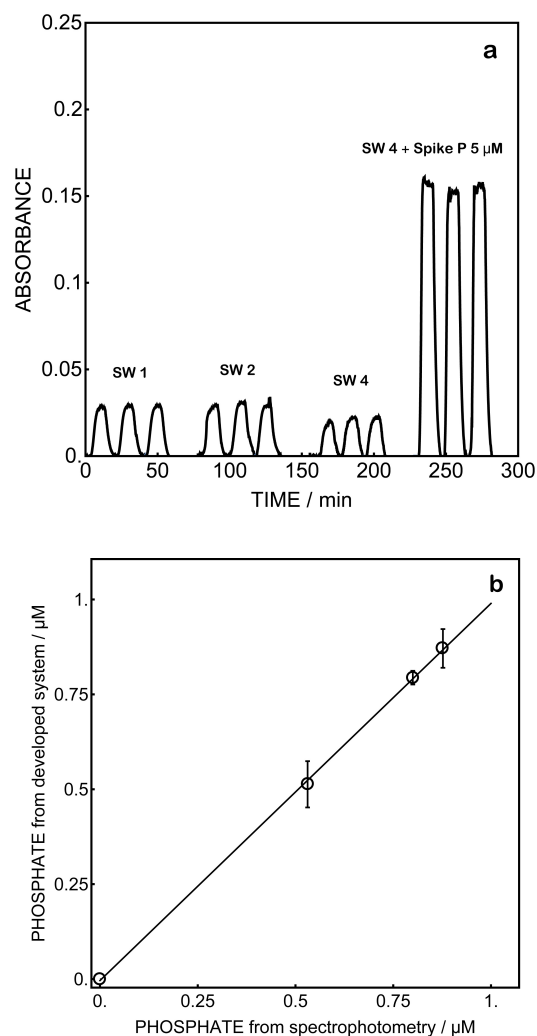


Figure 6. (a) Time-based responses for seawater samples containing different phosphate levels (SW1-SW4), (b) Correlation graph between phosphate concentration obtained using developed system and phosphate determined by standard spectrophotometry, volume of sample plug ca. 1 ml. Absorbance is measured at 660 nm.

electrochemical detection of the resulting phosphomolybdate complex, the more established spectrophotometric detection was chosen here to best assess the performance of the membrane modules. The associated time profiles for samples containing varying levels of phosphate in a 0.6 M

NaCl are presented in Figure 5 (Top). Linearity was obtained in the range of 0.1-10 μM phosphate, see Figure 5 (Bottom).

Silicate is known to be the principal interferent in the molybdenum blue method as it also forms heteropoly acids (12-MSA/12-molybdosilicic acid, $\text{H}_4\text{SiMo}_{12}\text{O}_{40}$), thereby reducing available molybdenum blue concentration.¹⁰ Generally, silicate concentration in aquatic systems is in the submicromolar range. Silicate concentration required for siliceous phytoplankton such as diatoms is <0.1-0.6 μM in the euphotic zone.^{8,30} From the literature, it is suggested that silicate interference can be suppressed with high acidity or using antimonyl tartrate as the source of Sb(III).⁴ Here, organic acid was used in the combined reductant reagent (potassium antimonyl tartrate), as tartaric acid may help to minimise silicate interference. From the result shown in Figure S9, adding 10 μM silicate solution to a 1 μM phosphate solution does not significantly interfere. Only excessive silicate concentrations not common for most seawater environments give interference.

The in-line membrane system was applied to the determination of phosphate concentration in a range of unmodified seawater samples as shown in Figure 6a. Phosphate concentrations of (0.794 ± 0.018) , (0.871 ± 0.051) , and (0.513 ± 0.061) μM were detected in the samples, see Table S1. The phosphate concentrations in the same samples were also determined by the traditional molybdate assay chosen as reference method. The resulting cross-correlation is shown in Figure 6b. The data from the two methods are in a good agreement, although we note that the phosphate level in seawater sample 3 was too low to be detectable with either method.

CONCLUSIONS

An in-line flow system employing ion-exchange membrane-based reagent delivery was successfully developed for the determination of inorganic phosphate in seawater. The performance of the ion-exchange membranes was acceptable and showed no dramatic loss of phosphate through the membrane modules. The device was coupled to spectrophotometric detection for seawater measurement, demonstrating the detection of phosphate levels as low as 0.1 μM . The key advantage of this approach is a simpler, more integrated membrane-based reagent delivery principle, compared to established approaches that rely on mixing. While the long-term goal of this research is to develop a miniaturized sensing device with integrated electrochemical detection, the spectrophotometric detection chosen here is an intermediate milestone that lends itself well to the validation of the membrane-based delivery principle.

ASSOCIATED CONTENT

Supporting Information

The Supporting Information is available free of charge on the ACS Publications website.

Detailed illustration of the custom-made modules, schematic diagram of on-line configuration with spectrophotometric detection, voltammetric experiment with paper-based cell,

molybdenum calibration, correlation between molybdenum in the feed and in the resulting sample, evaluation of molybdenum loss within H-module, FAPQ membrane selectivity study via potentiometric experiment with FAPQ-based electrode. Effect of flow rate, solution volume, molybdate concentration and silicate interference on the absorbance signal. Results of phosphate determination in seawater samples and validation by standard spectrophotometry. Table S1, Figures S1-S9 (PDF).

AUTHOR INFORMATION

Corresponding Author

* Email address: eric.bakker@unige.ch

Author Contributions

‡These authors contributed equally.

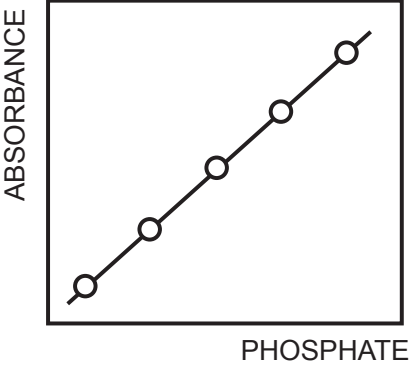
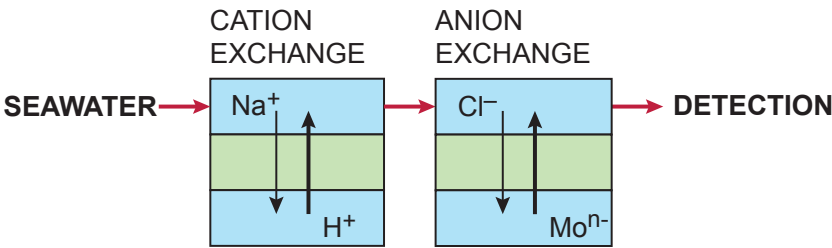
ACKNOWLEDGMENT

The authors thank the Swiss National Science Foundation (SNSF) and the University of Geneva for financial support of this study. The Science Achievement Scholarship of Thailand (SAST) is acknowledged for the scholarship to Suphasinee Sateanchok. The authors thank Marylou Tercier-Waeber (University of Geneva) for her valuable assistance with the seawater samples used in this work.

REFERENCES

- (1) Estela, J. M.; Cerda, V., Flow analysis techniques for phosphorus: an overview. *Talanta* **2005**, *66*, 307-331.
- (2) McDowell, R. W.; Hamilton, D. P., Nutrients and eutrophication: introduction. *Mar. and Freshwater Res.* **2013**, *64*, iii-vi.
- (3) Smith, V. H.; Schindler, D. W., Eutrophication science: where do we go from here? *Trends Ecol. Evol.* **2009**, *24* (4), 201-207.
- (4) Jayawardane, B. M.; McKelvie, I. D.; Kolev, S. D., A paper-based device for measurement of reactive phosphate in water. *Talanta* **2012**, *100*, 454-460.
- (5) Law al, A. T.; Adeloju, S. B., Progress and recent advances in phosphate sensors: A review. *Talanta* **2013**, *114*, 191-203.
- (6) Paytan, A.; McLaughlin, K., The Oceanic Phosphorus Cycle. *Chem. Rev.* **2007**, *107*, 563-576.
- (7) Matthew, D. P.; Rijkenberg, M. J. A.; Statham, P. J.; Stinchcombe, M. C.; Achterberg, E. P.; Mowlem, M., Determination of nitrate and phosphate in seawater at nanomolar concentrations. *Trends Anal. Chem.* **2008**, *27*, 169-182.
- (8) Ma, J.; Adornato, L.; Byrne, R. H.; Yuan, D., Determination of nanomolar levels of nutrients in seawater. *Trends Anal. Chem.* **2014**, *60*, 1-15.
- (9) Watanabe, M.; Ohtsu, J.; Otsuki, A., Daily Variations in Nutrient Concentrations of Seawater at 321 m Depth in Toyama Bay, Japan Sea. *J. Oceanogr.* **2000**, *56*, 553-558.
- (10) Nagul, E. A.; McKelvie, I. D.; Worsfold, P.; Kolev, S. D., The molybdenum blue reaction for the determination of orthophosphate revisited: Opening the black box. *Anal. Chim. Acta* **2015**, *890*, 60-82.
- (11) Murphy, J.; Riley, J. P., A modified single solution method for the determination of phosphate in natural waters. *Anal. Chim. Acta* **1962**, *27*, 31-36.
- (12) Strickland, J. D. H.; Parsons, T. R., A practical handbook of seawater analysis; Ottawa, Canada, 1972; p. 310.
- (13) Zhang, J. Z.; Fischer, C. J.; Ortner, P. B., Optimization of performance and minimization of silicate interference in continuous flow phosphate analysis. *Talanta* **1999**, *49*, 293-304.
- (14) Jonca, J.; Leon Fernandez, V.; Thouron, D.; Paulmier, A.; Graco, M.; Garçon, V., Phosphate determination in seawater: toward an autonomous electrochemical method. *Talanta* **2011**, *87*, 161-167.
- (15) Gray, S.; Hanrahan, G.; McKelvie, I.; Tappin, A.; Tse, F.; Worsfold, P., Flow Analysis Techniques for Spatial and Temporal Measurement of Nutrients in Aquatic Systems. *Environ. Chem.* **2006**, *3*, 3-18.
- (16) McKelvie, I. D.; Peat, D. M. W.; Worsfold, P. J., Techniques for the Quantification and Speciation of Phosphorus in Natural Waters. *Anal. Proc. incl. Anal. Commun.* **1995**, *32*, 437-445.
- (17) Jońca, J.; Giraud, W.; Barus, C.; Comtat, M.; Striebig, N.; Thouron, D.; Garçon, V., Reagentless and silicate interference free electrochemical phosphate determination in seawater. *Electrochim. Acta* **2013**, *88*, 165-169.
- (18) Barus, C.; Romanytsia, I.; Striebig, N.; Garçon, V., Toward an in situ phosphate sensor in seawater using Square Wave Voltammetry. *Talanta* **2016**, *160*, 417-424.
- (19) Ogawara, S.; Carey, J. L.; Zou, X. U.; Bühlmann, P., Donnan Failure of Ion-Selective Electrodes with Hydrophilic High-Capacity Ion-Exchanger Membranes. *ACS Sens.* **2016**, *1*, 95-101.
- (20) Afshar, M. G.; Crespo, G. A.; Bakker, E., Counter electrode based on an ion-exchanger Donnan exclusion membrane for bioelectroanalysis. *Biosens. Bioelectron.* **2014**, *61*, 64-69.
- (21) Grygolowicz-Pawlak, E.; Crespo, G. A.; Afshar, M. G.; Mislberger, G.; Bakker, E., Potentiometric sensors with ion-exchange Donnan exclusion membranes. *Anal. Chem.* **2013**, *85*, 6208-6212.
- (22) Pankratova, N.; Cuartero, M.; Cherubini, T.; Crespo, G. A.; Bakker, E., In-Line Acidification for Potentiometric Sensing of Nitrite in Natural Waters. *Anal. Chem.* **2017**, *89*, 571-575.
- (23) Pankratova, N., Development of Sensing Principles for Electrochemical Detection of Nutrients and Species Relevant to the Carbon Cycle; Doctoral Thesis, University of Geneva, 2018; p. 112-129.
- (24) Cuartero, M.; Pankratova, N.; Cherubini, T.; Crespo, G. A.; Massa, F.; Confalonieri, F.; Bakker, E., In Situ Detection of Species Relevant to the Carbon Cycle in Seawater with Submersible Potentiometric Probes. *Environ. Sci. & Technol. Lett.* **2017**, *4*, 410-415.
- (25) Cuartero, M.; Crespo, G. A.; Bakker, E., Paper-based thin-layer coulometric sensor for halide determination. *Anal. Chem.* **2015**, *87*, 1981-1990.
- (26) Bakker, E., Determination of Unbiased Selectivity Coefficients of Neutral Carrier-Based Cation-Selective Electrodes. *Anal. Chem.* **1997**, *69*, 1061-1069.
- (27) Chester, R.; Jickells, T., Marine Geochemistry, 3rd edition; John Wiley & Sons: Oxford, 2012; p. 411.
- (28) Cuartero, M.; Crespo, G. A.; Bakker, E., Tandem electrochemical desalination-potentiometric nitrate sensing for seawater analysis. *Anal. Chem.* **2015**, *87*, 8084-8089.
- (29) Ruzicka, J.; Hansen E.H., Flow Injection Analysis; A Wiley-Interscience Publication, USA, 1988; p. 15-36.
- (30) Brzezinski, M. A.; Nelson, D. M., A solvent extraction method for the colorimetric determination of nanomolar concentrations of silicic acid in seawater. *Mar. Chem.* **1986**, *19*, 139-151.

FOR TOC ONLY



Supporting Information for

In-Line Seawater Phosphate Detection with Ion-Exchange Membrane Reagent Delivery

Suphasinee Sateanchok^{a,b}, Nadezda Pankratova^a, Maria Cuartero^a, Thomas Cherubini^a, Kate Grudpan^b and Eric Bakker^{a}*

^a Department of Inorganic and Analytical Chemistry, University of Geneva, Quai Ernest-Ansermet 30, CH-1211 Geneva, Switzerland

^b Center of Excellence for Innovation in Analytical Science and Technology, Chiang Mai University, Chiang Mai 50200, Thailand, and Department of Chemistry, Faculty of Science, Chiang Mai University, Chiang Mai 50200, Thailand

Figures

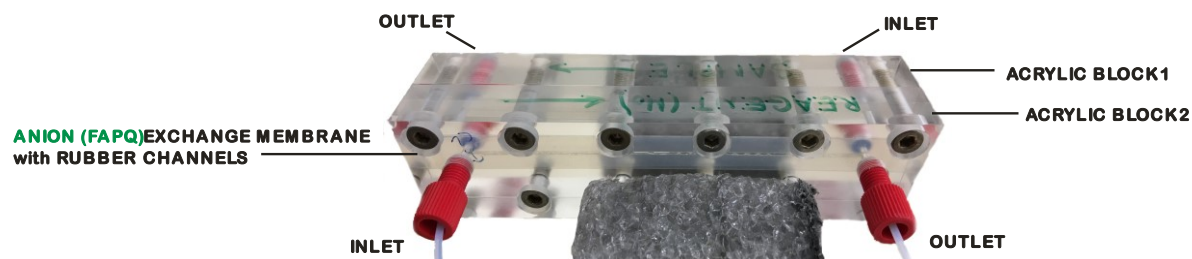


Figure S1. Schematic illustration of the custom-made module for membrane delivery: inlet, outlet, acrylic block, rubber channel. Anion-exchange membrane (FAPQ) are used for molybdate-module.

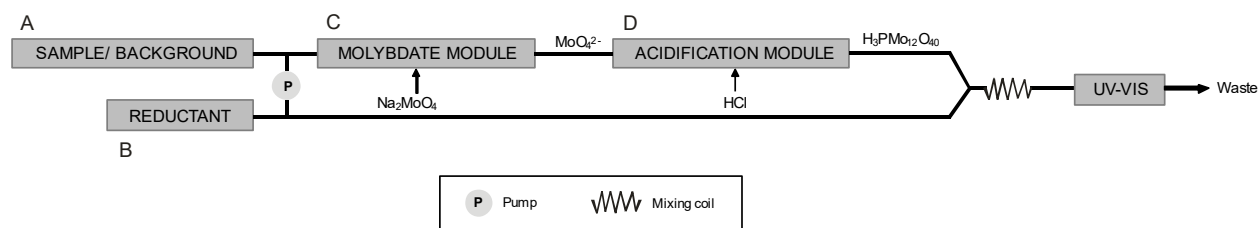


Figure S2. Schematic diagram of in-line configuration with spectrophotometric detection. The solution is delivered by peristaltic pumps at a flow rate of $90 \mu\text{L min}^{-1}$. The flow is directed from left to right until the analyzed solution is collected in waste bottles.

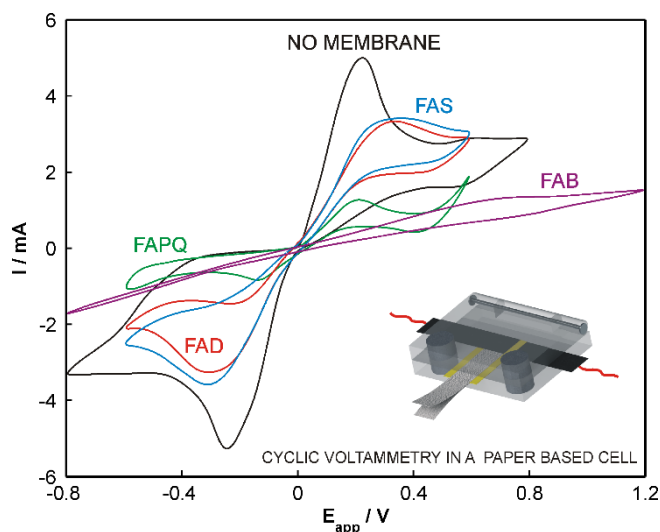


Figure S3. Cyclic voltammograms obtained at 5 mV/s scan rate* in a paper-based cell with and without (black) anion-exchange membrane: Ag|AgCl|NaCl 100 mM|Membrane|NaCl 100 mM|Ag. Membrane = FAB-PK-130 (purple), FAS-PET-130 (blue), FAD-PET-75 (red), FAPQ-375-PP (green).

* The CV for the FAB membrane presented here refers (exceptionally) to the scan rate 10 mV/s.

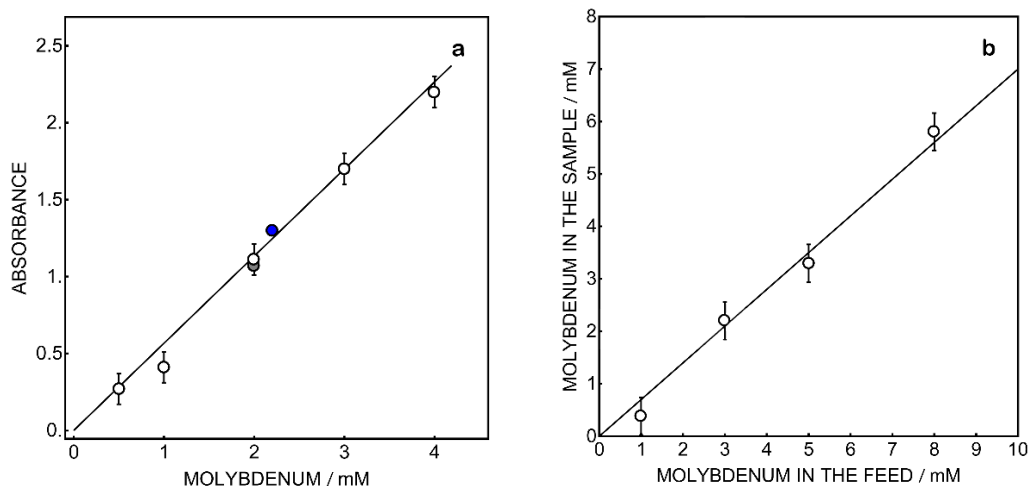


Figure S4. Molybdenum detection at 660 nm in the UV flow cell. (a, white circles) Calibration line obtained using colorimetric method by passing molybdate calibration solutions with 0.6 M NaCl background, spiked with mixed reagent Reagent^(Mo), directly to UV detection (avoiding additional modules). (a, gray circle) Absorbance signal after passing the solution containing 2 mM molybdate through the H-module and subsequent spiking with mixed reagent (but containing no sulfuric acid) prior to the detection. (a, blue circle) Absorbance signal after passing the solution containing 3 mM molybdate through the Mo-module, then H-module and subsequent spiking with mixed reagent (but containing no sulfuric acid and molybdate) prior to the detection. (b) Molybdenum concentration detected colorimetrically (using calibration line shown in Figure S4a) at the outlet of the molybdate module vs initial molybdate concentration in the solution with 0.6 M NaCl background.

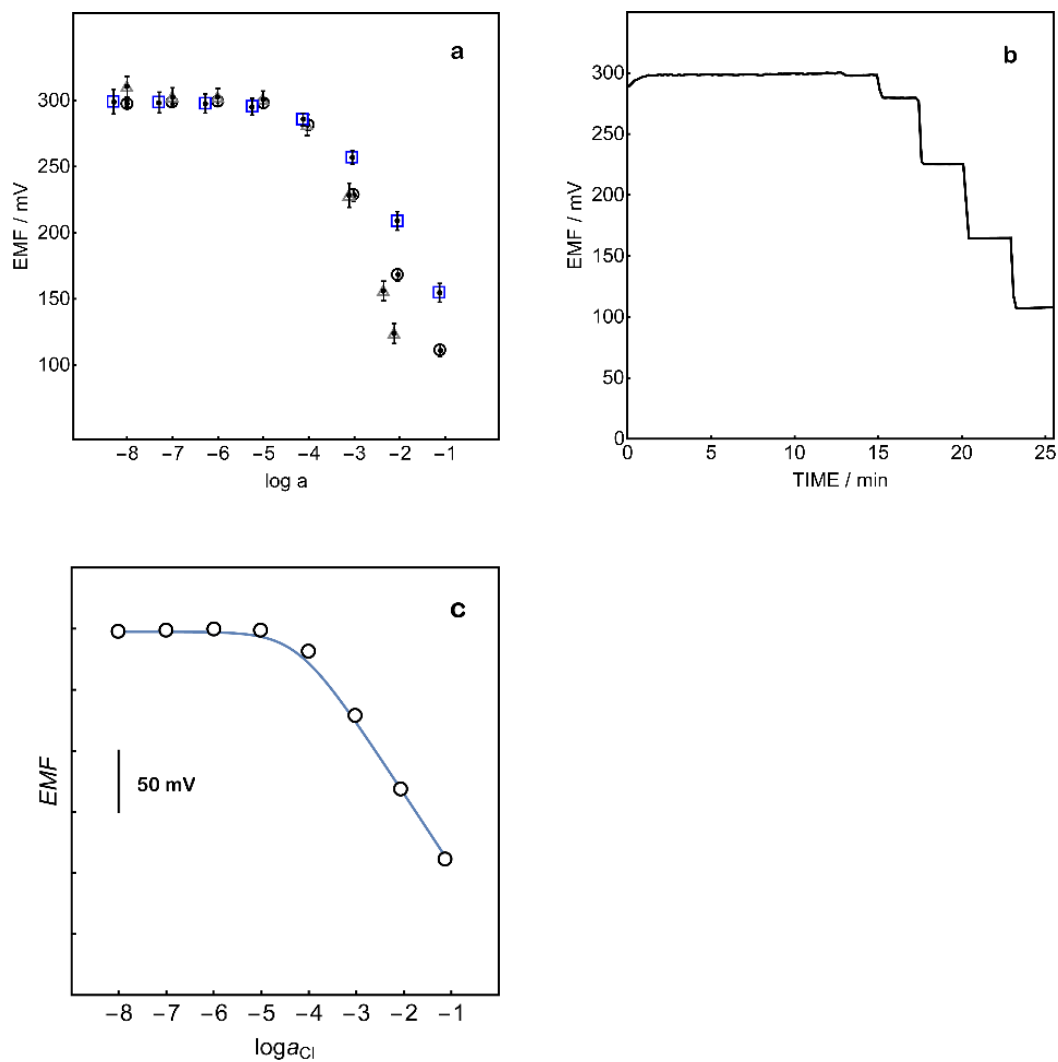


Figure S5. (a) Experimental data points (error bars are standard deviations) for the EMF responses of FAPQ-based electrodes for different anions: Cl^- (black circle), MoO_4^{2-} (gray triangle), and H_2PO_4^- (blue square). FAPQ (anion-exchange) membrane was conditioned in NaCl 0.6 M and the inner solution was 10 mM of NaCl. (b) Associated EMF time-trace upon NaCl addition, obtained with a FAPQ-based electrode. (c) Potentiometric calibration curve upon NaCl addition, obtained with a FAPQ-based electrode.

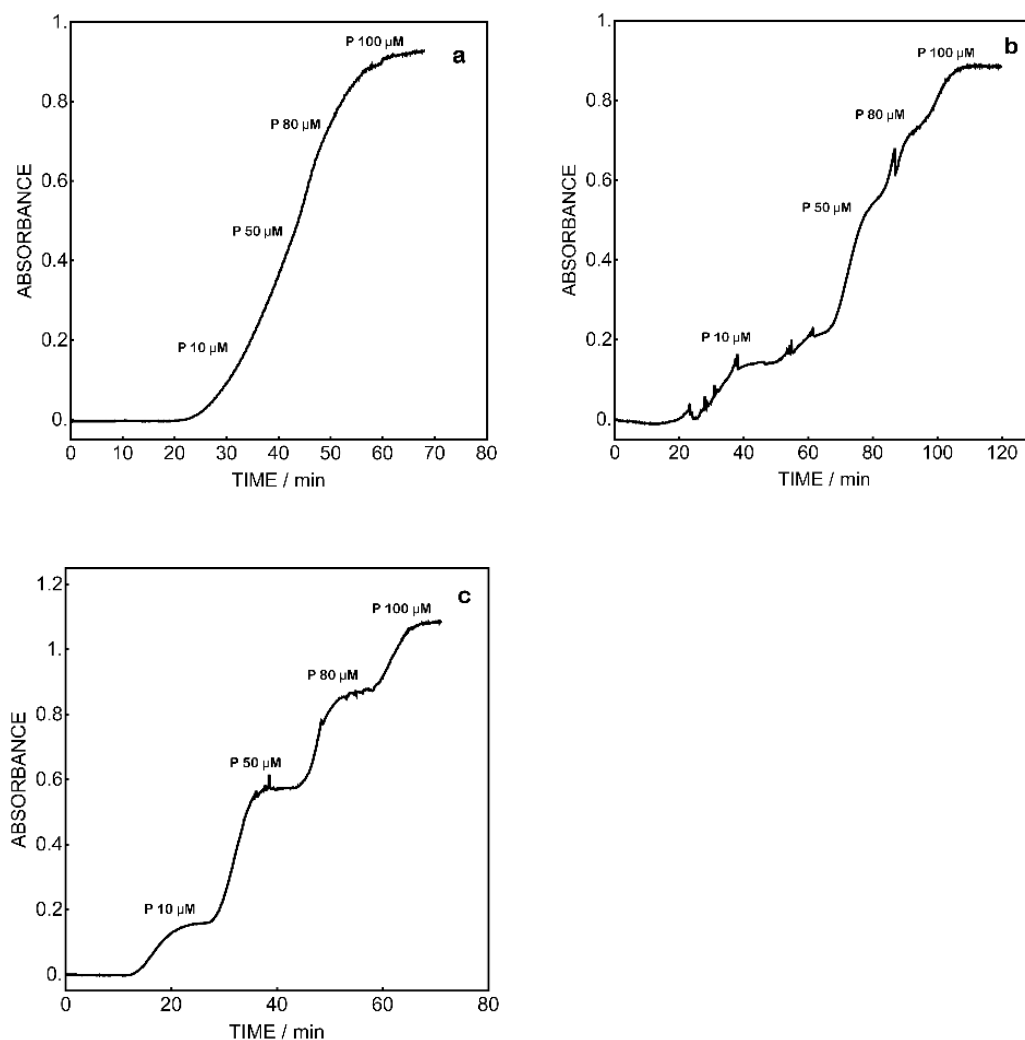


Figure S6. Absorbance vs time response for different flow rates: (a) 20 $\mu\text{L min}^{-1}$, (b) 45 $\mu\text{L min}^{-1}$ and (c) 90 $\mu\text{L min}^{-1}$, phosphate concentration 0-100 μM . Phosphate detection was achieved at 660 nm in a flow-through cell directly connected to UV/Vis spectrophotometer (see experimental section). 5-6 M HCl and 3 mM molybdate solutions were fed into the H-module and Mo-module respectively.

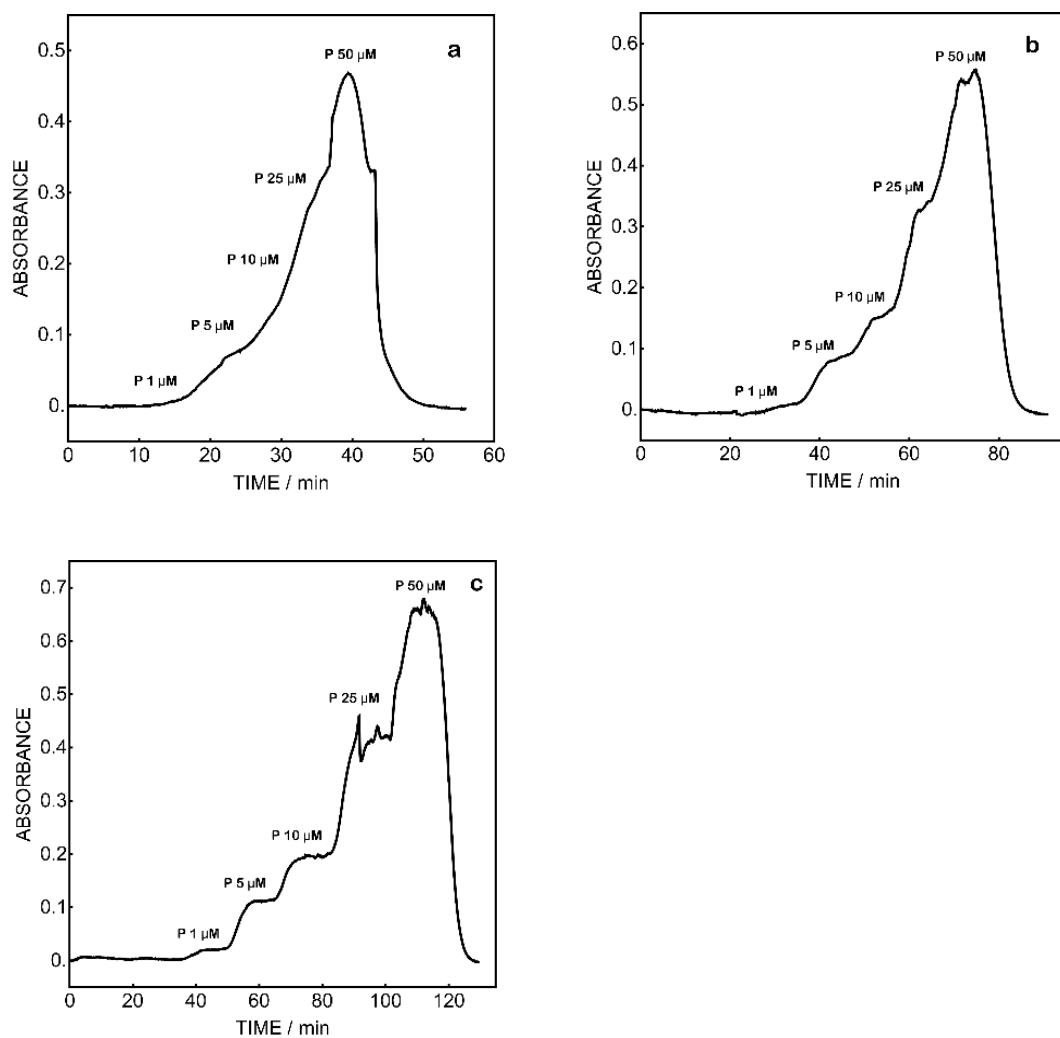


Figure S7. Absorbance vs time response for different solution volumes: (a) 0.45 mL, (b) 1 mL and (c) 1.35 mL, phosphate concentration 0-50 μM . Phosphate detection was achieved at 660 nm in a flow-through cell directly connected to UV/Vis spectrophotometer (see experimental section). 5-6 M HCl and 3 mM molybdate solutions were fed into the H-module and Mo-module respectively.

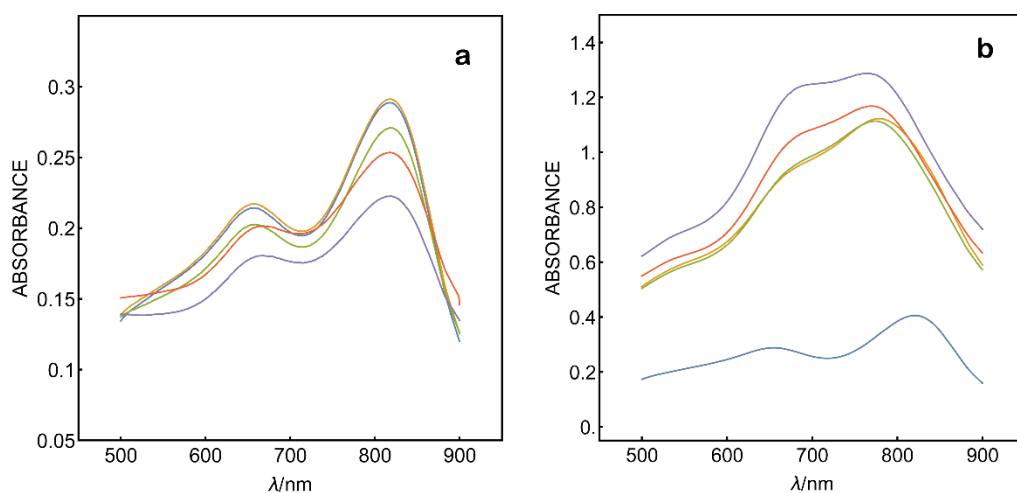


Figure S8. Absorbance scan spectrum for phosphate detection with different molybdenum concentrations: (a) 10 μM phosphate, (b) 100 μM phosphate. Lines of different colors correspond to different concentrations of molybdate: 3, 6, 10, 16 and 20 mM.

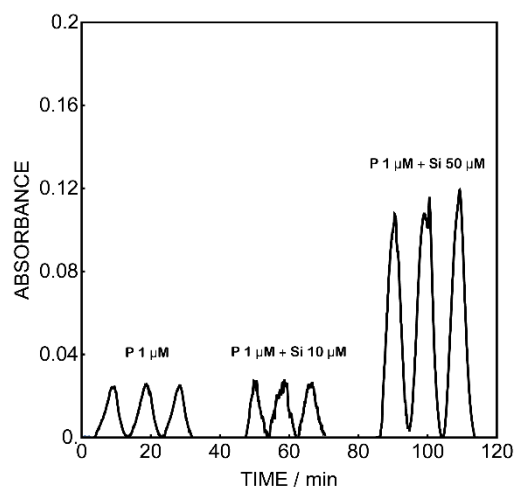


Figure S9. Absorbance vs time response illustrating silicate interference in phosphate determination, volume of sample plug ca. 0.45 ml. Phosphate concentration 1 μM was spiked with silicate to study the interference effect. Absorbance of blue complex was measured at 660 nm in a flow-through cell directly connected to UV/Vis spectrophotometer (see experimental section).

Table

Table S1. Phosphate analysis in seawater samples (n=3)

Sample	Developed method (μM Phosphate)	Spectrophotometry (μM Phosphate)
SW1	0.794 ± 0.018	0.800 ± 0.027
SW2	0.871 ± 0.051	0.877 ± 0.035
SW3	ND*	ND*
SW4	0.513 ± 0.061	0.531 ± 0.043
SW4 + spike P 5 μM	5.701 ± 0.094	5.615 ± 0.039
P 3.5 μM^{**}	-	3.553 ± 0.080
P 1 μM^{**}	-	1.185 ± 0.044

* ND: not detected

** For checking the performance of spectrophotometric method using known concentration of phosphate